Available online at www.sciencedirect.com
ScienceDirect
Chinese Journal of Aeronautics 22(2009) 371-379
Chinese Journal of Aeronautics
www.elsevier.com/locate/cja

Dynamics Model of Carrier-based Aircraft Landing Gears Landed on Dynamic Deck

Zhang Wen*, Zhang Zhi, Zhu Qidan, Xu Shiyue

Department of Automation, Harbin Engineering University, Harbin 150001, China

Received 1 July 2008; accepted 8 October 2008

Abstract

In order to study the carrier-based aircraft landing laws landed on the carrier, the dynamics model of carrier-based aircraft landing gears landed on dynamic deck is built. In this model, the interactions of the carrier-based aircraft landing attitude and the damping force acting on landing gears are considered, and the influence of dynamic deck is introduced into the model through the deck normal vectors. The wheel-deck coordinate system is put forward to solve the complex simulation problem of force-on-wheel which comes from the dynamic deck. At last, by simulation, it is demonstrated that the model can be applied to landing attitude when the carrier-based aircraft is landing on the dynamic deck, it is also proved that the model is comprehensive and suitable for any abnormal landing situation.

Keywords: carrier-based aircraft; landing gear; deck; wheel-deck coordinate system; landing

1. Introduction

During landing task, the landing gears of carrier-based aircraft are landed on the deck with six degrees of freedom (six-DOF) motion. Therefore there will be various relative aircraft landing velocities and attitudes with respect to the dynamic deck, which result in the landing gears being landed in various dissymmetric situations. Consequently, the compressing status of the landing gear damper for landing on the deck is more complex than that for landing on the ground[1-3].

Over a long period of time, most studies on landing gears model are based on ground landing aircraft[4-8]. As there is so little dissymmetric ground landing, in these models the aircraft attitude and the comprehensive actions between landing gears and fuselage are ignored[9-13]. The landing gears model based on the carrier-based aircraft is very few, and most of them ignore the aircraft attitude influence and focus on the landing impact.

In this article the dynamics model of carrier-based aircraft landing gears is built, and the model will be applied to the study of the landing criteria for aircraft carrier (CV). In this model the aircraft landing velocity and attitude, which are relative to the dynamic deck, are taken into account. The model can be used to analyze the landing gears impact which is the fundamental study concerning the safety of landing.

2. Computation Scheme

Fig.1 illustrates the definition of the basic coordinate systems.

The ground coordinate system $O_g x_g y_g z_g$ (represented by S_g) is fixed to the ground. The origin O_g is a point located on the ground, axis z_g is in the plumb downward direction, axis x_g is in the level and related to the flight tasks. And axes x_g, y_g, and z_g follow the right-hand rule.

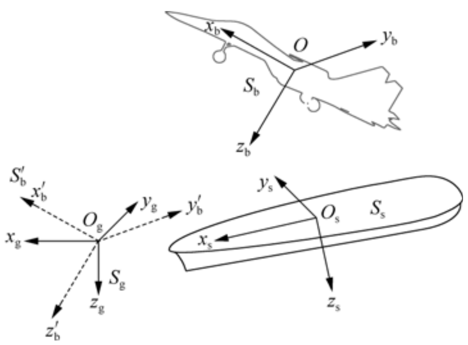

Fig.1 Sketch of carrier-based aircraft coordinate systems.

*Corresponding author. Tel.: +86-13624602760.
E-mail address: ziye560922@126.com

doi:10.1016/S1000-9361(08)60113-2

$Ox_by_bz_b$ (represented by S_b) is the aircraft-body coordinate system which is fixed to the airframe. The origin O is placed at the aircraft mass center. Along the longitudinal axis of aircraft, the positive direction of x_b is directed towards the prow. Axis z_b is in the aircraft symmetry plane downward vertically. And axis y_b is perpendicular to the aircraft symmetry plane pointing to the right-hand direction. Furthermore, aircraft-body-fixed ground coordinate system $O_g x'_b y'_b z'_b$ (represented by S'_b) is defined, its origin is O_g, and axes x'_b, y'_b, and z'_b parallel the axes x_b, y_b, and z_b respectively. Without consideration of position displacement of the aircraft, S'_b would coincide with S_b.

$O_s x_s y_s z_s$ (represented by S_s) is the carrier-body coordinate system which is fixed to the carrier. The origin O_s is placed at the carrier mass center. Axis x_s is in the longitudinal central plane of the carrier and parallel to waterline plane pointing to the prow, axis y_s is perpendicular to the longitudinal central plane and parallel to waterline plane pointing to the starboard, and axis z_s is in the longitudinal central plane and perpendicular to the waterline plane pointing to the bottom. Also, the carrier-body-fixed ground coordinate system (represented by S'_s) $O_g x'_s y'_s z'_s$ is defined, its origin is placed at O_g, and its axes parallel the axes of S_s respectively. Without consideratin of position displacement of the carrier, S'_s would coincide with S_s.

In this article the randomness, which attributes to the various relative landing attitudes of carrier-based aircraft, is taken into account. In other words, the carrier-based aircraft attitude and the carrier attitude are considered concurrently. Therefore, during the landing task, three landing gears may be landed with any possible conditions, and the axes of landing gear struts would be in any possible attitudes. Moreover, after touchdown the trend of jumping and shimmying for the aircraft may be complex. Summing up all the above mentional features, the particularity of the modeling task in this article is as follows.

(1) Under different landing conditions, there may be various landing attitudes of the carrier-based aircraft, and result in different deck reaction forces which act on the wheel. Consequently, the aircraft landing attitude is an indispensable factor to be considered in the force-on-wheel model.

(2) Besides the complex landing attitude of the carrier-based aircraft, the deck attitude is also varying during landing. In this article by acquiring the deck normal vector of the touchdown point, the direction of the deck vertical force-on-wheel is gained. Thereby, the influence of the moving deck reaction force on the landing gear is reflected, and the influences of the aircraft attitudes on the deck force-on-wheel can be presented synthetically.

(3) It is indispensable to simulate the six-DOF differential equation of carrier-based aircraft and the differential equations of three dampers. In this way, the model can adapt to the landing conditions in which the relative aircraft attitude and the relative landing velocity are arbitrary, and the dynamic interactions between the fuselage and landing gears are presented.

The deck reaction forces act on the fuselage through landing gears, when the aircraft is landing on the deck. Taking landing gear i ($i = 1,2,3$) as an example, the forces acting on the aircraft during touchdown are analyzed. In the following text, i (i=1,2,3) indicates the left main landing gear, right main landing gear, and nose landing gear respectively. As shown in Fig.2, deck vertical force-on-wheel $F_{i,z}$ is translated into damping force $F_{i,s}$ through the landing gear damper system. In other words, $F_{i,s}$ which acts upon the fuselage is caused by the deck vertical force $F_{i,z}$ (aiming at strut damper system). The rolling friction force $F_{i,x}$ and the sliding friction force $F_{i,y}$, which act on the wheel, are in the deck plane, and can be named as sectional forces. Since the damper cannot cushion the sectional forces, the sectional forces can be passed to the fuselage directly. To transform the sectional forces to S_s, $F_{i,xb}$ and $F_{i,yb}$ are obtained. To sum up, the landing gear forces, acting on the fuselage, include $F_{i,s}$, $F_{i,xb}$, and $F_{i,yb}$. In Fig.2, θ is pitching angle of aircraft.

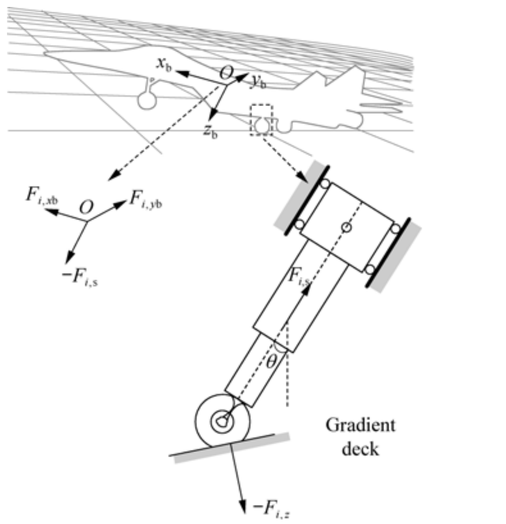

Fig.2 Force analyses of landing carrier-based aircraft.

3. Wheel-deck Coordinate System

3.1. Presentation of wheel-deck coordinate system

As shown in Fig.3(a), the deck vertical force $F_{i,z}$ parallels the axis z_s, the rolling friction force $F_{i,x}$ is along the direction of wheel course, and the sliding friction force $F_{i,y}$ is perpendicular to $F_{i,z}$ and $F_{i,x}$. These three forces follow the right-hand rule and can constitute a coordinate system. It should be noted that $F_{i,x}$ and $F_{i,y}$ are parallel to axes x_b and y_b respectively, when there are no aircraft pitching and rolling angles. $F_{i,x}$ and $F_{i,y}$ will not be parallel to axes x_b and y_b, when the aircraft pitching and rolling angles are not zero; they will be along the direction of x_b; y_b projections on the deck plane respectively.

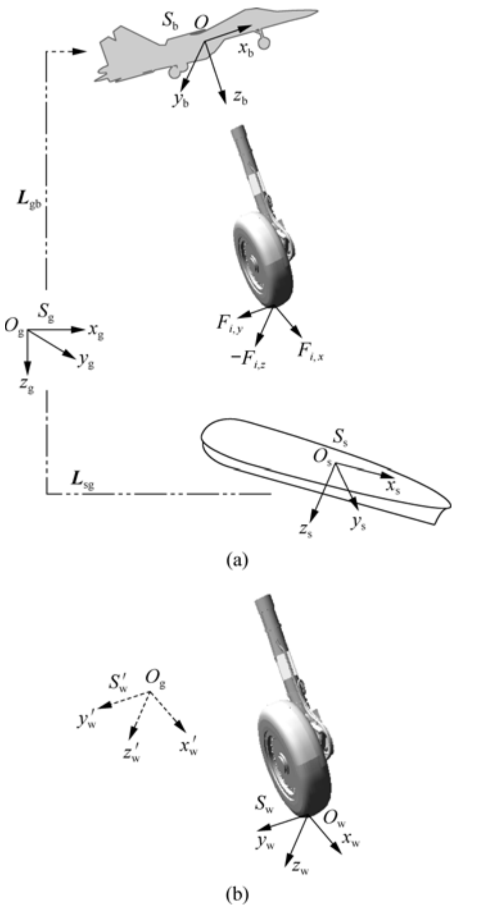

Fig.3 Schematic diagrams of wheel-deck coordinate systems.

When the wheel friction force is being calculated, the relative wheel velocities along the directions of wheel course and wheel axis are needed, and they are the wheel velocities being relative to the deck velocity. However, in this model, the deck velocity and wheel velocity are in the form of S_s and S_b components. To acquire the relative wheel velocity, it is indispensable to decompose the deck velocity and wheel velocity into the directions of wheel course and the wheel axis. Similarly, in subsequent modeling process, the forces which act on the deck should be decomposed into other coordinate systems. It is obvious that the directions of $F_{i,x}$ and $F_{i,y}$ are independent of any defined coordinate due to the aircraft attitude. In such case, the modeling process would be very complex. Therefore, a new coordinate system should be introduced and the axes of the new coordinate system should be parallel to the directions of the forces which act on the deck. With the new coordinate transformation matrix, the above modeling process will be simplified.

Since the new coordinate system is correlated with the deck and the wheel, it can be named as wheel-deck coordinate system. As shown in Fig.3(b), the wheel-deck coordinate system $O_w x_w y_w z_w$ (represented by S_w) is fixed to the wheel, and its origin is O_w which is the point nearest to the wheel center in the contact surface of wheel and deck. Axis x_w is along the wheel course, axis z_w is parallel to z_s pointing to the deck, and axis y_w is perpendicular to x_w and y_w following the right-hand rule. Moreover, the wheel-fixed ground coordinate system $O_g x'_w y'_w z'_w$ (represented by S'_w) is defined, its origin is O_g and axes x'_w, y'_w, and z'_w are parallel to axes x_w, y_w, and z_w respectively. Without consideration of position displacement of the wheel, S'_w would coincide with S_w.

In Fig.3, $\boldsymbol{L}_{gb}$ is the transformation matrix which transforms S_g into S'_b, and $\boldsymbol{L}_{sg}$ is the transformation matrix which transforms S'_s into S_g. They are given by Eqs.(1)-(2).

$$\boldsymbol{L}_{gb}=\begin{bmatrix} C_\theta C_\psi & C_\psi S_\theta S_\phi - S_\psi C_\phi & C_\psi S_\theta C_\phi + S_\psi S_\phi \\ S_\psi C_\theta & S_\psi S_\theta S_\phi + C_\psi C_\phi & S_\psi S_\theta C_\phi - C_\psi S_\phi \\ -S_\theta & C_\theta S_\phi & C_\theta C_\phi \end{bmatrix} \quad (1)$$

$$\boldsymbol{L}_{sg}=\begin{bmatrix} C_\Theta C_\Psi & C_\Theta S_\Psi & -S_\Theta \\ S_\Phi S_\Theta C_\Psi - C_\Phi S_\Psi & S_\Phi S_\Theta S_\Psi + C_\Phi C_\Psi & S_\Phi C_\Theta \\ C_\Phi S_\Theta C_\Psi + S_\Phi S_\Psi & C_\Phi S_\Theta S_\Psi - S_\Phi C_\Psi & C_\Phi C_\Theta \end{bmatrix} \quad (2)$$

where $C_\cdot = \cos(\cdot)$ and $S_\cdot = \sin(\cdot)$; ψ and ϕ are the aircraft yawing angle and rolling angle respectively; Ψ, Θ, and Φ are the carrier azimuth, pitching angle, and rolling angle respectively.

3.2. Acquisition of wheel-deck coordinate system

$\boldsymbol{f}_g=\begin{bmatrix}\boldsymbol{i}_g\\ \boldsymbol{j}_g\\ \boldsymbol{k}_g\end{bmatrix}$ and $\boldsymbol{f}'_w=\begin{bmatrix}\boldsymbol{i}'_w\\ \boldsymbol{j}'_w\\ \boldsymbol{k}'_w\end{bmatrix}$ are the vector arrays of S_g and S'_w respectively. The axes directions of S'_w are varying all the time, because they are depending on the wheel attitude. In the vector array $\boldsymbol{f}'_w$, $\boldsymbol{k}'_w$ represents the direction of deck normal vector for point O_w. As the carrier landing deck is straight and flat, the directions of deck normal vectors for point O_w and carrier mass center are identical, and they are given by

$$\boldsymbol{k}'_w = \boldsymbol{L}_{sg}\begin{bmatrix}0\\0\\1\end{bmatrix} \quad (3)$$

$$\boldsymbol{j} = \boldsymbol{L}_{sg}\boldsymbol{L}_{gb}\begin{bmatrix}0\\1\\0\end{bmatrix} \quad (4)$$

where $\boldsymbol{j}$ is the vector of axis y_b. As mentioned above, $\boldsymbol{j}'_w$ is the projection of $\boldsymbol{j}$ on the deck plane. Since the plane determined by $\boldsymbol{j}$ and $\boldsymbol{k}'_w$ is parallel to the plane determined by $\boldsymbol{j}'_w$ and $\boldsymbol{k}'_w$, $\boldsymbol{i}'_w$ can be represented by

$$\boldsymbol{i}'_w = \boldsymbol{j}\times\boldsymbol{k}'_w \quad (5)$$

According to the right-hand rule, $\boldsymbol{j}'_w$ can be acquired by $\boldsymbol{k}'_w$ and $\boldsymbol{i}'_w$

$$\boldsymbol{j}'_{\mathrm{w}} = \boldsymbol{k}'_{\mathrm{w}} \times \boldsymbol{i}'_{\mathrm{w}} \tag{6}$$

The acquired $\boldsymbol{i}'_{\mathrm{w}}$, $\boldsymbol{j}'_{\mathrm{w}}$, and $\boldsymbol{k}'_{\mathrm{w}}$ may not be the unit vectors, so it is needed to be unitized before using.

$\boldsymbol{L}_{\mathrm{wg}}$ is the transformation matrix which transforms S'_{w} into S_{g}, and can be obtained by the transformation of component arrays

$$\boldsymbol{L}_{\mathrm{wg}} = \begin{bmatrix} \boldsymbol{i}'_{\mathrm{w}} \bullet \boldsymbol{i}_{\mathrm{g}} & \boldsymbol{i}'_{\mathrm{w}} \bullet \boldsymbol{j}_{\mathrm{g}} & \boldsymbol{i}'_{\mathrm{w}} \bullet \boldsymbol{k}_{\mathrm{g}} \\ \boldsymbol{j}'_{\mathrm{w}} \bullet \boldsymbol{i}_{\mathrm{g}} & \boldsymbol{j}'_{\mathrm{w}} \bullet \boldsymbol{j}_{\mathrm{g}} & \boldsymbol{j}'_{\mathrm{w}} \bullet \boldsymbol{k}_{\mathrm{g}} \\ \boldsymbol{k}'_{\mathrm{w}} \bullet \boldsymbol{i}_{\mathrm{g}} & \boldsymbol{k}'_{\mathrm{w}} \bullet \boldsymbol{j}_{\mathrm{g}} & \boldsymbol{k}'_{\mathrm{w}} \bullet \boldsymbol{k}_{\mathrm{g}} \end{bmatrix} \tag{7}$$

4. Modeling

In order to show the interactions among the landing gears, the deck, and the fuselage, it is necessary to build the force and damper model of landing gears and the carrier-based aircraft fuselage motion model. Then, on the basis of these models and introducing the deck motion model, the dynamics model of carrier-based aircraft landing gears landing on dynamic deck is acquired.

4.1. Force and damper model of landing gears

The force and damper model of landing gears adopts the classical two-mass model which divideds the aircraft into two parts: the elastic supporting part which is the portion above the air spring of damper, with its mass center at the aircraft trunnion (represented by T_1); and the inelastic supporting part which is the portion below the air spring of damper with its mass center as the wheel center (represented by T_2). The modeling processes of force-on-wheel model and damper model are as follows.

(1) Force-on-wheel model

The force-on-wheel model includes the wheel deck-detection model and the wheel force calculation model, the modeling processes are significantly simplified well by wheel-deck coordinate system.

① Contact-detection model of wheel and deck

For the complex relative attitude between the aircraft and the deck in landing, wheel compression amount is acquired by the contact-detection of wheel and deck. On this basis, the deck force-on-wheel can be gained. In fact, the wheel compression amount is the distance between the position of T_2 measured in S_{s} and the wheel radius. Thus, it can be given by

$$\begin{bmatrix} x_{T_2 i,\mathrm{s}} \\ y_{T_2 i,\mathrm{s}} \\ z_{T_2 i,\mathrm{s}} \end{bmatrix} = \boldsymbol{L}_{\mathrm{sg}} \left(\boldsymbol{L}_{\mathrm{gb}} \begin{bmatrix} x_{T_2 i,\mathrm{b}} \\ y_{T_2 i,\mathrm{b}} \\ z_{T_2 i,\mathrm{b}} \end{bmatrix} - \begin{bmatrix} x_{\mathrm{c,g}} \\ y_{\mathrm{c,g}} \\ z_{\mathrm{c,g}} \end{bmatrix} \right) \tag{8}$$

$$\delta_i = \begin{cases} R_i - (-z_{T_2 i,\mathrm{s}}) & \begin{array}{c} R_i + z_{T_2 i,\mathrm{s}} \geq 0 \text{ and} \\ x_{T_2 i,\mathrm{s}} \text{ and } y_{T_2 i,\mathrm{s}} \text{are in} \\ \text{the area of the deck} \end{array} \\ 0 & \text{else} \end{cases} \tag{9}$$

where $x_{T_2 i,\mathrm{b}}$, $y_{T_2 i,\mathrm{b}}$, and $z_{T_2 i,\mathrm{b}}$ are the T_2 coordinate representations of landing gear i in S_{b}; $x_{T_2 i,\mathrm{s}}$, $y_{T_2 i,\mathrm{s}}$, and $z_{T_2 i,\mathrm{s}}$ the T_2 coordinate representations of landing gear i in S_{s}; R_i and δ_i the wheel radius and the wheel compression amount respectively; and $x_{\mathrm{c,g}}$, $y_{\mathrm{c,g}}$, and $z_{\mathrm{c,g}}$ the coordinate representations of the carrier in S_{g}.

② Force-on-wheel calculation model

The force-on-wheel can be acquired under the condition of knowing the wheel compression amount. The relative velocity between the wheel center T_2 and the deck is needed to be determinal, when the wheel sectional forces are calculated. The numerically value of relative velocity in S_{w} and in S'_{w} are identical, so for the sake of convenience, the relative velocity is calculated in S'_{w} in this article. Furthermore, the relative velocities along the wheel course direction and the wheel axial direction are ignored, in that the landing gear motion along both directions are the fuselage motion along these directions. According to the semi- empirical theory[14], the force-on-wheel can be calculated as follows:

$$F_{i,z} = (1 + C_{\delta_i} \dot{\delta}_i) C_i \delta_i \tag{10}$$

$$F_{i,x} = \mu_i F_{i,z} \left[1 - \exp(-\phi_{i,x} - E_{i,y} \phi_{i,x}^3) \right] \tag{11}$$

$$F_{i,y} = \mu_i F_{i,z} \left[1 - \exp(-\phi_{i,y} - E_{i,y} \phi_{i,y}^3) \right] \tag{12}$$

$$\phi_{i,y} = \frac{K_i \tan \lambda_i}{\mu_i (1 + C_{\delta_i} \dot{\delta}_i) C_i \delta_i} \tag{13}$$

$$\phi_{i,x} = \frac{K_{i,x} S_{i,x}}{\mu_i (1 + C_{\delta_i} \dot{\delta}_i) C_i \delta_i} \tag{14}$$

$$\lambda_i = \arctan \frac{v'_{T_2 i,x\mathrm{w}} - v'_{\mathrm{c},x\mathrm{w}}}{v'_{T_2 i,y\mathrm{w}} - v'_{\mathrm{c},y\mathrm{w}}} \tag{15}$$

$$\begin{bmatrix} v'_{T_2 i,x\mathrm{w}} \\ v'_{T_2 i,y\mathrm{w}} \\ v'_{T_2 i,z\mathrm{w}} \end{bmatrix} = \boldsymbol{L}_{\mathrm{wg}} \boldsymbol{L}_{\mathrm{gb}} \begin{bmatrix} v'_{T_2 i,x\mathrm{b}} \\ v'_{T_2 i,y\mathrm{b}} \\ v'_{T_2 i,z\mathrm{b}} \end{bmatrix} \tag{16}$$

$$v'_{T_2 i,y\mathrm{b}} = v'_{\mathrm{p},y\mathrm{w}} \tag{17}$$

$$v'_{T_2 i,z\mathrm{b}} = v'_{\mathrm{p},z\mathrm{w}} \tag{18}$$

$$\begin{bmatrix} v'_{\mathrm{p},x\mathrm{w}} \\ v'_{\mathrm{p},y\mathrm{w}} \\ v'_{\mathrm{p},y\mathrm{w}} \end{bmatrix} = \boldsymbol{L}_{\mathrm{wg}} \boldsymbol{L}_{\mathrm{gb}} \begin{bmatrix} v'_{\mathrm{p},x\mathrm{b}} \\ v'_{\mathrm{p},y\mathrm{b}} \\ v'_{\mathrm{p},z\mathrm{b}} \end{bmatrix} \tag{19}$$

$$\begin{bmatrix} v'_{\mathrm{c},x\mathrm{w}} \\ v'_{\mathrm{c},y\mathrm{w}} \\ v'_{\mathrm{c},z\mathrm{w}} \end{bmatrix} = \boldsymbol{L}_{\mathrm{wg}} \begin{bmatrix} v'_{\mathrm{c},x\mathrm{g}} \\ v'_{\mathrm{c},y\mathrm{g}} \\ v'_{\mathrm{c},z\mathrm{g}} \end{bmatrix} \tag{20}$$

where $v_{\mathrm{c},\,x\mathrm{g}}$, $v_{\mathrm{c},\,y\mathrm{g}}$, and $v_{\mathrm{c},\,z\mathrm{g}}$ are the velocity components of carrier in S_{g}; $v'_{\mathrm{c},\,x\mathrm{w}}$, $v'_{\mathrm{c},\,y\mathrm{w}}$, and $v'_{\mathrm{c},\,z\mathrm{w}}$ the velocity components of carrier in S'_{w}; $v'_{\mathrm{p},\,x\mathrm{b}}$, $v'_{\mathrm{p},\,y\mathrm{b}}$, and $v'_{\mathrm{p},\,z\mathrm{b}}$ the velocity components of the aircraft in S'_{b}; $v'_{\mathrm{p},\,x\mathrm{w}}$, $v'_{\mathrm{p},\,y\mathrm{w}}$, and $v'_{\mathrm{p},\,z\mathrm{w}}$ the velocity components of aircraft along axes x'_{w}, y'_{w}, and z'_{w} respectively; $v'_{T_2 i,x\mathrm{w}}$, $v'_{T_2 i,y\mathrm{w}}$, and

$v'_{T_2i,zw}$ the velocity components of T_2 in S'_w; $v'_{T_2i,xb}$, $v'_{T_2i,yb}$, and $v'_{T_2i,zb}$ the velocity components of T_2 in S'_b; $K_{i,x}$ is the wheel longitudinal rigidity; K_i the wheel cornering stiffness without lateral declination; $S_{i,x}$ the slip ratio; $E_{i,y}$ the transition coefficient; μ_i the adhesion coefficient; C_{δ_i} the wheel vertical damping deformation coefficient; and C_i the recombination damping coefficient.

Using the transformation of wheel-deck coordinate system, sectional forces $F_{i,xb}$ and $F_{i,yb}$ are obtained by transforming the three deck forces mentioned above into S_b

$$\begin{bmatrix} F_{i,xb} \\ F_{i,yb} \\ F_{i,zb} \end{bmatrix} = \boldsymbol{L}_{bg}\boldsymbol{L}_{wg}^{-1}\begin{bmatrix} F_{i,x} \\ F_{i,y} \\ F_{i,z} \end{bmatrix} \tag{21}$$

(2) Damper model

In order to obtain the compression amount of damper by the relative axial motion between T_1 and T_2, the equations of T_2 axial motion are established in the damper model. Then, the damping force is obtained with classical damper model.

① Calculation of the damper compression state

Damping force depends on the damper compression state variable U_i, and U_i is also the relative motion amount between the wheel and the fuselage, in other words, it is the relative axial motion between T_1 and T_2. There is no relative motion between T_1 and fuselage, and the axial motion of T_2 can be obtained through the axial forces ($F_{i,s}$ and $F_{i,zb}$). It should be noted that S_b is not the inertial system with respect to axial force, so $v'_{T_2i,zb}$, the axial velocity of T_2 in S'_b, has to be given first, then the axial velocity of T_2 in S_b is gained indirectly through the relative velocity of T_2 between S_b and S'_b. Ignoring the gravity of T_2, the damper compression state is given by

$$\frac{\mathrm{d}z_{T_2i,b}}{\mathrm{d}t} = v'_{T_2i,zb} - v_{T_2i,\bar{z}} \tag{22}$$

$$\frac{\mathrm{d}v'_{T_2i,zb}}{\mathrm{d}t} = \frac{F_{i,s} + F_{i,zb}}{m_{T_2i}} \tag{23}$$

$$\begin{bmatrix} v_{T_2i,\bar{x}} \\ v_{T_2i,\bar{y}} \\ v_{T_2i,\bar{z}} \end{bmatrix} = \begin{bmatrix} v'_{p,xb} \\ v'_{p,yb} \\ v'_{p,zb} \end{bmatrix} + \begin{bmatrix} \omega_{p,yb}z_{T_2i,b} - \omega_{p,zb}y_{T_2i,b} \\ \omega_{p,zb}x_{T_2i,b} - \omega_{p,xb}z_{T_2i,b} \\ \omega_{p,xb}y_{T_2i,b} - \omega_{p,yb}x_{T_2i,b} \end{bmatrix} \tag{24}$$

$$z_{T_1i,b} = h_i \tag{25}$$

$$U_i = z_{T_2i,b} - z_{T_1i,b} \tag{26}$$

where $\omega_{p,xb}$, $\omega_{p,yb}$, and $\omega_{p,zb}$ are aircraft angular velocity components in S_b; $z_{T_1i,b}$ is the coordinate component of T_1 along axis z_b; and h_i the distance between aircraft mass center and aircraft trunnion.

② Damping force calculation

As mentioned above, the deck vertical force-on-wheel is transferred to the fuselage through the damper, and influences the aircraft attitude. At the same time, the damping force reacts on the elastic supporting part and influences the position of this part. So, the role of damping force is very important in the whole model. Its calculation processes are as follows.

For landing gear i, the damping force $F_{i,s}$ includes the air spring force F_{ai}, the oleo-damping force F_{hi}, and the internal frictional force F_{fi} (ignoring the external friction)[15] as shown in Eq.(27). Taking single cavity-single cylinder damper as an example, the damping force is given by

$$F_{i,s} = F_{ai} + F_{hi} + F_{fi} \tag{27}$$

$$F_{ai} = S_{ai}(P_{Bi} - P_{atm}) = S_{ai}\left[P_{B0i}\left(\frac{V_{B0i}}{V_{B0i} - S_{ai}U_i}\right)^{\gamma_i} - P_{atm}\right] \tag{28}$$

$$F_{hi} = S_{hi}(P_{Ai} - P_{Bi})\frac{\rho S_{hi}{}^2\dot{U}_i}{2S_{di}{}^2C_{di}^2}\left|\dot{U}_i\right| \tag{29}$$

Ignoring the strut bending, Eq.(30) is achieved.

$$F_{fi} = \pi\mu_{bi}D_{bi}H_{bi}(P_{Bi} - P_{atm})\frac{\dot{U}_i}{\left|\dot{U}_i\right|} \tag{30}$$

where P_{atm}, P_{Bi}, P_{B0i}, and P_{Ai} are the atmospheric pressure, the instantaneous pressure of low pressure cavity, the initial pressure of low pressure, and the instantaneous pressure of high pressure cavity respectively; S_{ai}, S_{hi}, and S_{di} the external sectional area of the piston rod, the internal net area of piston rod, and net area of oil hole respectively; γ_i, ρ, C_{di}, μ_{bi}, D_{bi}, and H_{bi} the polytropic exponent of air compress process, the oil density, the coefficient of oil contraction, the friction coefficient and diameter of the inner surface of outer cylinder, and the height of piston ring respectively; and V_{B0i} is the initial volume of low pressure cavity.

4.2. Fuselage motion model of carrier-based aircraft

The motion of fuselage can be divided into the parallel translation motion and the rotation motion of mass center, so the equations of the fuselage motion are as follows.

The parallel translation motion equation of mass center is[16-18]

$$\begin{bmatrix} \dfrac{\mathrm{d}v'_{p,xb}}{\mathrm{d}t} \\ \dfrac{\mathrm{d}v'_{p,yb}}{\mathrm{d}t} \\ \dfrac{\mathrm{d}v'_{p,zb}}{\mathrm{d}t} \end{bmatrix} = \begin{bmatrix} \omega_{p,zb}v'_{p,yb} - \omega_{p,yb}v'_{p,zb} \\ \omega_{p,xb}v'_{p,zb} - \omega_{p,zb}v'_{p,xb} \\ \omega_{p,yb}v'_{p,xb} - \omega_{p,xb}v'_{p,yb} \end{bmatrix} + \frac{\sum \boldsymbol{F}}{m} \tag{31}$$

$$\begin{bmatrix} \dfrac{\mathrm{d}x_{p,g}}{\mathrm{d}t} \\ \dfrac{\mathrm{d}y_{p,g}}{\mathrm{d}t} \\ \dfrac{\mathrm{d}z_{p,g}}{\mathrm{d}t} \end{bmatrix} = \boldsymbol{L}_{gb}\begin{bmatrix} v'_{p,xb} \\ v'_{p,yb} \\ v'_{p,zb} \end{bmatrix} \tag{32}$$

The rotation motion equation is

$$\begin{bmatrix} \dfrac{\mathrm{d}\omega_{\mathrm{p},x\mathrm{b}}}{\mathrm{d}t} \\ \dfrac{\mathrm{d}\omega_{\mathrm{p},y\mathrm{b}}}{\mathrm{d}t} \\ \dfrac{\mathrm{d}\omega_{\mathrm{p},z\mathrm{b}}}{\mathrm{d}t} \end{bmatrix} = \begin{bmatrix} \dfrac{(I_z^2 + I_{xz}^2 - I_z I_y)\omega_{\mathrm{p},z\mathrm{b}}\omega_{\mathrm{p},x\mathrm{b}} - I_{xz}(I_x + I_z - I_y)\omega_{\mathrm{p},y\mathrm{b}}\omega_{\mathrm{p},x\mathrm{b}}}{I_x I_z - I_{xz}{}^2} \\ \dfrac{(I_x - I_z)\omega_{\mathrm{p},z\mathrm{b}}\omega_{\mathrm{p},x\mathrm{b}} + I_{xz}(\omega_{\mathrm{p},x\mathrm{b}}^2 - \omega_{\mathrm{p},z\mathrm{b}}^2)}{I_y} \\ \dfrac{(I_x I_y - I_{xz}^2 - I_x^2)\omega_{\mathrm{p},y\mathrm{b}}\omega_{\mathrm{p},x\mathrm{b}} - I_{xz}(I_y - I_x - I_z)\omega_{\mathrm{p},z\mathrm{b}}\omega_{\mathrm{p},y\mathrm{b}}}{I_x I_z - I_{xz}{}^2} \end{bmatrix} + \begin{bmatrix} \dfrac{I_z}{I_x I_z - I_{xz}{}^2} & 0 & \dfrac{I_{xz}}{I_x I_z - I_{xz}{}^2} \\ 0 & \dfrac{1}{I_y} & 0 \\ \dfrac{I_{xz}}{I_x I_z - I_{xz}{}^2} & 0 & \dfrac{I_x}{I_x I_z - I_{xz}{}^2} \end{bmatrix} \sum \boldsymbol{M} \tag{33}$$

$$\begin{bmatrix} \dfrac{\mathrm{d}\phi}{\mathrm{d}t} \\ \dfrac{\mathrm{d}\theta}{\mathrm{d}t} \\ \dfrac{\mathrm{d}\psi}{\mathrm{d}t} \end{bmatrix} = \begin{bmatrix} \omega_{\mathrm{p},x\mathrm{b}} + \tan\theta(\omega_{\mathrm{p},y\mathrm{b}}\sin\phi + \omega_{\mathrm{p},z\mathrm{b}}\cos\phi) \\ \omega_{\mathrm{p},y\mathrm{b}}\cos\phi - \omega_{\mathrm{p},z\mathrm{b}}\sin\phi \\ \dfrac{(\omega_{\mathrm{p},y\mathrm{b}}\sin\phi + \omega_{\mathrm{p},z\mathrm{b}}\cos\phi)}{\cos\theta} \end{bmatrix} \tag{34}$$

where I_x, I_y, and I_z are the aircraft inertia moments in S_{b}; I_{xz} is the aircraft inertia product in S_{b}; m the mass of the aircraft; $\sum \boldsymbol{F}$ and $\sum \boldsymbol{M}$ are respectively the resultant force vector and the resultant moment vector.

During the landing, the forces and moments include gravity $\boldsymbol{G}$, aerodynamic force $\boldsymbol{F}_{\mathrm{a,b}}$ and moment $\boldsymbol{M}_{\mathrm{a,b}}$, engine thrust $\boldsymbol{F}_{\mathrm{t,b}}$ and moment $\boldsymbol{M}_{\mathrm{t,p}}$, and the force $\boldsymbol{F}_{i,\mathrm{b}}$ and corresponding moment $\boldsymbol{M}_{i,\mathrm{b}}$ acting on the fuselage through landing gear i. The resultant force and moment are given by

$$\sum \boldsymbol{F} = \boldsymbol{G} + \boldsymbol{F}_{\mathrm{a,b}} + \boldsymbol{F}_{\mathrm{t,b}} + \sum_{i=1}^{3} \boldsymbol{F}_{i,\mathrm{b}} \tag{35}$$

$$\sum \boldsymbol{M} = \boldsymbol{M}_{\mathrm{a,b}} + \boldsymbol{M}_{\mathrm{t,b}} + \sum_{i=1}^{3} \boldsymbol{M}_{i,\mathrm{b}} \tag{36}$$

$$\boldsymbol{F}_{i,\mathrm{b}} = \begin{bmatrix} F_{i,x\mathrm{b}} \\ F_{i,y\mathrm{b}} \\ F_{i,\mathrm{s}} \end{bmatrix} \tag{37}$$

$$\boldsymbol{M}_{i,\mathrm{b}} = \begin{bmatrix} 0 \\ 0 \\ F_{i,\mathrm{s}} \end{bmatrix} \boldsymbol{h}_{qi} + \begin{bmatrix} F_{i,x\mathrm{b}} \\ F_{i,y\mathrm{b}} \\ 0 \end{bmatrix} \boldsymbol{h}_i \tag{38}$$

where $\boldsymbol{h}_{\mathrm{q}i}$ and $\boldsymbol{h}_i$ are respectively the moment arm vectors of the damping force and the deck force with respect to aircraft mass center.

4.3. Dynamics model of carrier-based aircraft landing gears

The force and damper model and the fuselage motion model have been built already. In order to apply these models to the carrier-based aircraft landing simulation, it is indispensable to constitute the landing dynamics model of carrier-based aircraft.

The landing dynamic system of carrier-based aircraft involves the fuselage motion, the landing gear damper motion, and the deck motion. The system scale is large, and the interactions between every part are complex. In this article the state variable $\boldsymbol{C}$ of carrier six-DOF motion is taken as the system input, and the eighteen state variables are used to describe the dynamic process of the aircraft landing dynamics system. The eighteen state variables include twelve motional variables $v'_{\mathrm{p},x\mathrm{b}}$, $v'_{\mathrm{p},y\mathrm{b}}$, $v'_{\mathrm{p},z\mathrm{b}}$, $\omega_{\mathrm{p},x\mathrm{b}}$, $\omega_{\mathrm{p},y\mathrm{b}}$, $\omega_{\mathrm{p},z\mathrm{b}}$, $x_{\mathrm{p,g}}$, $y_{\mathrm{p,g}}$, $z_{\mathrm{p,g}}$, ϕ, θ, and ψ; the position variable $z_{T_2 i,\mathrm{b}}$ in T_2 and velocity variable $v'_{T_2 i,z\mathrm{b}}$ of landing gear in T_2. It is clear that the dimension of the system is high. For simplifying the system and making the system be more realizable, the system is divided into two correlative sub-models. Sub-model I is the carrier-based aircraft fuselage motion model which includes twelve variables of aircraft; Sub-model II is the force and damper model of landing gears which includes the position variables of T_2 and velocity variables of three landing gears. The two sub-models correlate with each other by the interacting forces between carrier-based aircraft and landing gears, the model is mathematically expressed as follows.

$$\begin{cases} \boldsymbol{x}_1 = [v'_{\mathrm{p},x\mathrm{b}} \quad v'_{\mathrm{p},y\mathrm{b}} \quad v'_{\mathrm{p},z\mathrm{b}} \quad \omega_{\mathrm{p},x\mathrm{b}} \quad \omega_{\mathrm{p},y\mathrm{b}} \\ \qquad \omega_{\mathrm{p},z\mathrm{b}} \quad x_{\mathrm{p,g}} \quad y_{\mathrm{p,g}} \quad z_{\mathrm{p,g}} \quad \phi \quad \theta \quad \psi]^{\mathrm{T}} \\ \boldsymbol{x}_2 = [z_{T_2 1,\mathrm{b}} \quad z_{T_2 2,\mathrm{b}} \quad z_{T_2 3,\mathrm{b}} \quad v'_{T_2 1,z\mathrm{b}} \quad v'_{T_2 2,z\mathrm{b}} \quad v'_{T_2 3,z\mathrm{b}}]^{\mathrm{T}} \end{cases}$$

Sub-model I: $$\dot{\boldsymbol{x}}_1 = \boldsymbol{f}_1(\boldsymbol{x}_1, \boldsymbol{\zeta}_{12}) \tag{39}$$

Sub-model II: $$\dot{\boldsymbol{x}}_2 = \boldsymbol{\zeta}_{21} \tag{40}$$

Correlation terms: $$\boldsymbol{\zeta}_{12} = \boldsymbol{F}_{i,\mathrm{b}} = \boldsymbol{g}_1(\boldsymbol{x}_1, \boldsymbol{x}_2, \boldsymbol{C}, \vartheta) \tag{41}$$

$$\boldsymbol{\zeta}_{21} = \boldsymbol{g}_2(\boldsymbol{F}_{i,\mathrm{b}}, \boldsymbol{x}_1) \tag{42}$$

Nonlinear function $\boldsymbol{f}_1(\bullet)$ is the integrated expression of Eqs.(31)-(38); nonlinear function $\boldsymbol{g}_1(\bullet)$ is defined by Eqs.(8)-(21) and Eqs.(25)-(30); nonlinear function $\boldsymbol{g}_2(\bullet)$ can be obtained through Eqs.(22)-(24).

As the carrier course and speed are constant, the system input $\boldsymbol{C}$, i.e. the state variable of carrier six-DOF motion, can be approximately written as

$$\boldsymbol{C} = \begin{bmatrix} x_{\mathrm{c,g}} \\ y_{\mathrm{c,g}} \\ z_{\mathrm{c,g}} \\ \Theta \\ \Phi \\ \Psi \end{bmatrix} = \begin{bmatrix} v_{\mathrm{c},x\mathrm{g}}t + A_x \sin(\omega_x t + \varphi_x) \\ v_{\mathrm{c},y\mathrm{g}}t + A_y \sin(\omega_y t + \varphi_y) \\ v_{\mathrm{c},z\mathrm{g}}t + A_z \sin(\omega_z t + \varphi_z) \\ A_\Theta \sin(\omega_\Theta t + \varphi_\Theta) \\ A_\Phi \sin(\omega_\Phi t + \varphi_\Phi) \\ 0 \end{bmatrix} \tag{43}$$

where the carrier swaying, surging, heaving, pitching, and rolling motions are approximately expressed as sinusoidal motions; A_x, A_y, A_z, A_Θ, and A_Φ are respectively the amplitude of carrier swaying, surging, heaving, pitching, and rolling; ω_x, ω_y, ω_z, ω_Θ, and ω_Φ respectively the frequency of swaying, surging, heaving, pitching, and rolling; and φ_x, φ_y, φ_z, φ_Θ, and φ_Φ respectively the initial phase of swaying, surging, heaving, pitching, and rolling.

5. Simulation and Results Analyses

The simulation of the landing gears dynamics model is realized by the combined development environment of VC and MATLAB, and the three- dimensional display environment of OpenGL. Though there are many attitude and motion situations of the carrier-based aircraft and the carrier in different landing conditions, only three typical simulation situations are given, as shown in Table 1 and the analysis and verification are focused on Situation I.

In order to verify that the model can be applied to landing simulation for all kinds of bad situations, the rolling angle before landing of carrier-based aircraft is big in Situation I. For making the simulation results be more intuitive, assume that the carrier attitude is invariable. In Situation I, the two main landing gears are landed asynchronously, the falling vibration of landing gears is violent, and the fuselage attitude variations are frequent; all these are caused by the big initial attitude of the aircraft and the carrier. In this process, the asymmetric landing of main landing gears brings acute change to fuselage attitude and the fuselage yawing change is due to the aerodynamic effects of fuselage rolling. Furthermore, the fuselage pitching angle is also changed a bit for the reason of carrier triming. The simulation curves shown in Fig.4 illustrate the whole process completely. Moreover, the dynamic changes of fuselage attitude, force-on-wheel, and landing gears are presented in Fig.5 vividly.

Table 1 Analyses of carrier-based aircraft landing processes

	Initial settings of landing	Dynamic landing process
Situation I	Initial carrier-based aircraft attitude: ϕ=25, θ=8° Invariable carrier attitude: Θ= 8°, Φ= −20°	The left main landing gear is landed on the deck→the nose landing gear is landed→the right main landing gear is landed→main landing gear is in the deck→off tendency→three landing gears approach to be stable
Situation II	Initial carrier-based aircraft pitching angle: 8° Carrier pitching parameters: A_Θ=5°, $\omega_\Theta=\frac{\pi}{5}$ rad/s, φ_Θ= 0 rad/s	Two main landing gears are landed simultaneously→ nose landing gear is landed→two main landing gears are deck-off→main landing gears are landed slowly again and the force of nose landing gear decreased→ three landing gears approach to be stable.
Situation III	Initial carrier-based aircraft pitching angle: 8° Carrier pitching parameters: A_Θ=10°, $\omega_\Theta=\frac{\pi}{5}$ rad/s, φ_Θ= 0 rad/s	Three landing gears are landed simultaneously→nose landing gear tends to be deck-off→three landing gears approach to be stable

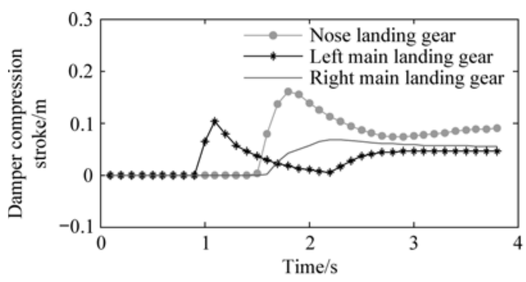

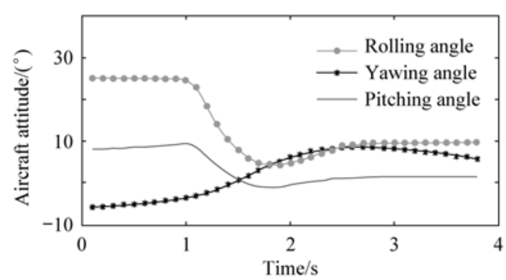

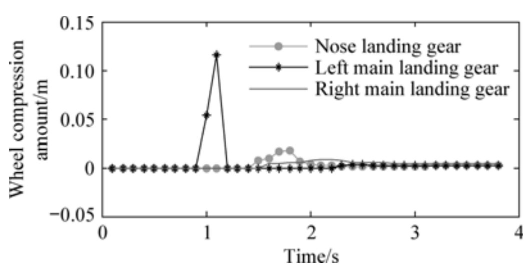

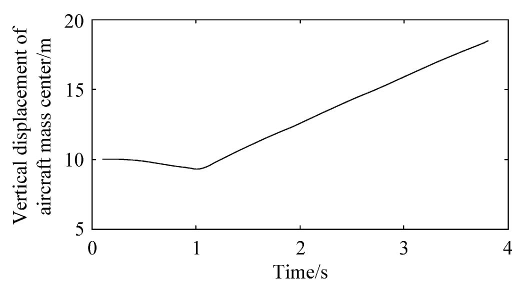

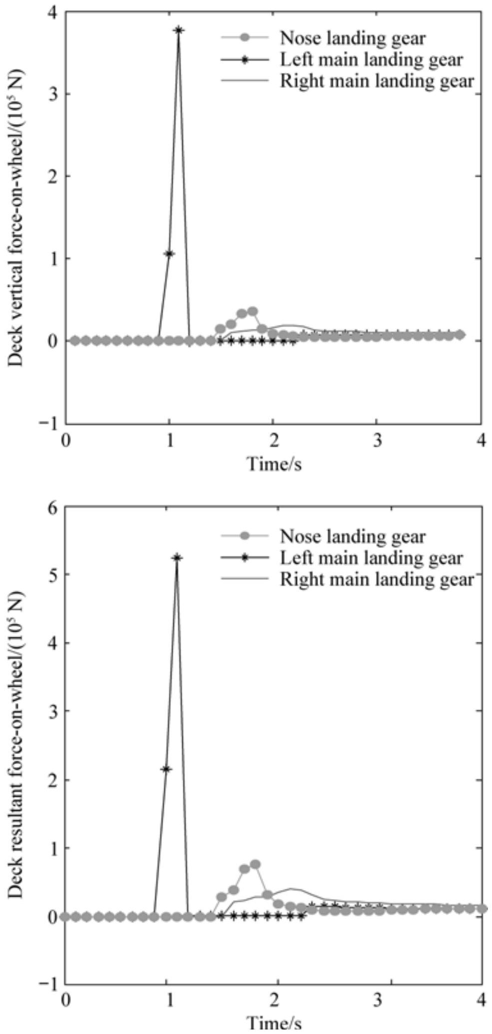

Fig.4 Simulation curves of carrier-based aircraft landing (Situation I).

The simulation curves of carrier-based aircraft landing processes for Situations II−III are shown in Fig.6.

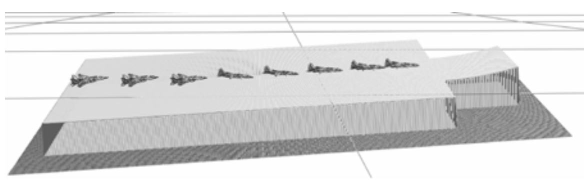

(a) Left view sketch

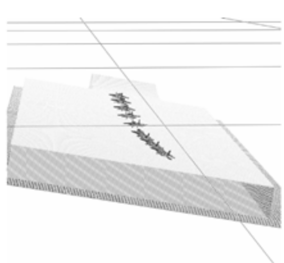

(b) Back view sketch

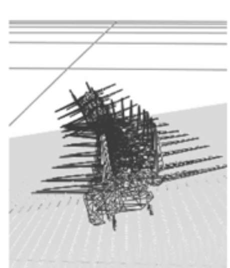

(c) Front view sketch

(d) Partial enlarged sketch

Fig.5 Simulation sketch of carrier-based aircraft landing (Situation I).

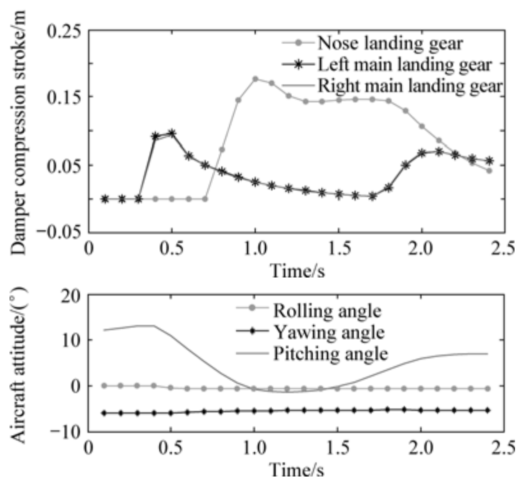

(a) Situation II

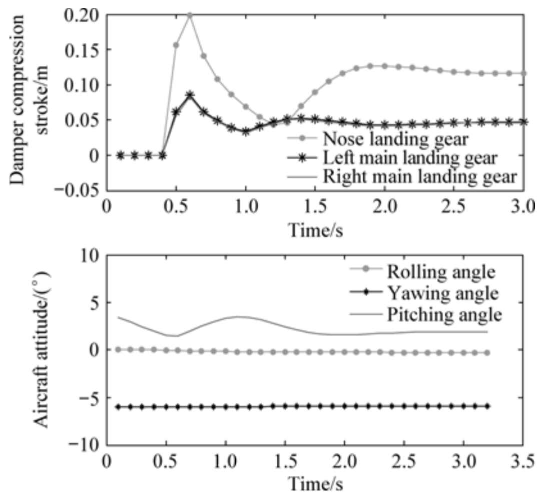

(b) Situation III

Fig.6 Simulation curves of carrier-based aircraft landing.

6. Conclusions

The simulation shows that the dynamics model of carrier-based aircraft landing gears given in this article can be applied to the dynamic process of carrier-based aircraft landing and can be utilized to simulate different landing situations with complex relative attitude between the carrier-based aircraft and the carrier. According to the analyses, the simulated landing processes conform to the actual processes and the model lays a foundation for the carrier-based aircraft landing simulation and the study of the deck landing safety. It can also serve the abnormal landing simulation of the conventional aircraft.

References

[1] Wei X H, Nie H. New method of attenuating landing impact force on carrier-based aircraft landing gear. Acta Aeronautica et Astronautica Sinica 2007; 28(2): 324-327. [in Chinese]

[2] W X H, Nie H. Study on landing impact force of carrier-based aircraft landing gear. China Mechanical Engineering 2007; 18(5): 520-523. [in Chinese]

[3] Liu W W, Qu X J. Mathematical model research on aircraft landing gear. Acta Aeronautica et Astronautica Sinica 2005; 18(4): 326-335. [in Chinese]

[4] Pritchard I J. An overview of landing gear dynamics. NASA TM-1999-209143, 1999.

[5] Somieski G. Shimmy analysis of a simple aircraft nose landing gear model using different mathematical methods. Aerospace Science and Technology 1997; 1 (8): 545-555.

[6] York B W, Alaverdi O. A physically representative aircraft landing gear model for real-time simulation. AIAA-96-3506, 1996.

[7] Atkinson C J. Development of an aerodynamic table lookup system and landing gear model for the CAL ploy flight simulator. PhD thesis, Aerospace Engineering Department, California Polytechnic State University, 2002.

[8] Yang C S, Huagn D. Study and analysis of dynamic simulation about airplane landing gear based on Matlab. Aeronautical Computing Technique 2006; 36(4): 96-99. [in Chinese]

[9] Gao Z J, Zhang R X. Mechanical model of landing impact of three dimensional fuselage landing gear. Acta Aeronautica et Astronautica Sinica 1991; 12(8): 327-349. [in Chinese]

[10] Xu D L, Li Y R. Mathematical model research on aircraft landing gear. Journal of System Simulation 2005; 17(4): 831-335. [in Chinese]

[11] Zhu J Y, Li L. Dynamics modeling and simulation of plane's landing gear. Journal of System Simulation 2005; 17(4): 831-835. [in Chinese]

[12] Cook F E, Milwitzky B. Effect of interaction on landing gear behavior and dynamic loads in a flexible airplane structure. NACA 1278, 1956.

[13] Liao L J, Jia Y H. Dynamic response simulation and analysis of landing gear with flexible fuselage. Acta Aeronautica et Astronautica Sinica 2008; 29(1): 75-78. [in Chinese]

[14] Guo K H. Vehicle manipulation dynamics. Changchun: Jilin Science & Technology Publishing House, 1992: 124-198. [in Chinese]

[15] Lin Y G, Cheng J L, Feng Z Y, et al. Parameter modeling and optimization analysis for landing gear absorber. Journal of System Simulation 2008; 20(10): 2732-2735. [in Chinese]

[16] Doyle G R, Jr. A review of computer simulation for aircraft-surface dynamics. Journal of Aircraft 1986; 23(4): 257-265.

[17] Yang X, Wang X H, Shen G Z, et al. Modeling and simulation research of six-degree-of-freedom fighter. Journal of System Simulation 2000; 12(3): 210-213. [in Chinese]

[18] Garza F R. A collection of nonlinear aircraft simulation. NASA TM-212145, 2003.

Biographies:

Zhang Wen Born in 1983, she is a Ph.D. candidate of Automation Department of Harbin Engineering University. Her main research interests are system simulation and control theory and engineering.
E-mail: ziye560922@126.com

Zhang Zhi Born in 1980, he received B.S. and M.S. degrees from Automation Department of Harbin Engineering University. His main research interests are system simulation and control theory and engineering.
E-mail: neverbadzz@163.com

Zhu Qidan Born in 1963, he received B.S. and M.S. degrees from Automation Department of Harbin Engineering University, and then became a teacher there. His main research interest is control theory and engineering.
E-mail: Zhuqd@public.hr.hl.cn

Xu Shiyue Born in 1984, she is a graduate student of Automation Department of Harbin Engineering University. Her main research interest is control theory and engineering.
E-mail: xsy2007@163.com